Modelling of Shear Localisation in Geomaterials

Lee, Jun-Seok*1
Pande, G. N*2
Pietruszczak. S*3

요 지

본 연구에서는 암반의 국부파괴 현상을 현실적으로 모형화하기 위하여 혼합체기법을 적용한 새로운 유한요소를 제안하였다. 이를 위하여 각 유한요소의 적분점에서 재료의 안정성을 검토하고 필요시 국부파괴 요소와 인접한 암반 물성을 이용한 혼합체 물성을 도출 하였으며 국부파괴 후의 재료 거동을 추적하였다.

제시한 모형을 사용하면 변형율 연화 모형을 사용하더라도 유한요소망의 객관성을 유지할 수 있으며 국부파괴 이후 재료의 거동을 현실적으로 모형화 할 수 있다. 또한 유한요소 갯수가 비교적 작더라도 수치해석 결과와 실험 결과가 잘 일치하고 있음을 알 수 있다.

Abstract

In this paper, an enhanced finite element model based on homogenisation technique is proposed to capture the localised failure mode of the intact rock masses. For this, bifurcation analysis at the element level is performed and, once the bifurcation is detected, equivalent material properties of the shear band and neighbouring intact rock are used to trace the post-peak behaviour of the material.

It is demonstrated that mesh sensitivity of the strain softening model is overcome and progressive failure mode of rock specimen can be simulated realistically. Furthermore, the numerical results show that the crack propagation and final failure mode can be captured with relatively coarse meshes and compares well with the experimental data available.

keywords : Shear localisation, Homogenisation technique, Strain-softening, Mesh sensitivity, Equivalent material properties

1. Introduction

Localisation of strains over a narrow region and formation of a shear band prior to collapse have been widely studied in recent years and various approaches and models have

*1 Member, Korea Highspeed Rail Construction Authority
*2 Professor, Department of Civil Engineering, University of Wales Swansea, U.K.
*3 Professor, Department of Civil Engineering, McMaster University, Canada

been proposed to overcome the numerical difficulties encountered with conventional analysis techniques such as finite elements, Here, Cosserat continuum model using additional rotational degree of freedom(Papanastasiou and Vardoulakis, 1992), gradient-dependent model employing higher degree of freedom(Borst and Pamin, 1996), visco-plastic model with length scale(Loret and Prevost, 1990), non-local model by way of a weighting function(Borst et al., 1993), enhanced finite element model adopting a special shape function (Steinmann and Willam, 1991), and adaptive mesh refinement technique(Ortiz and Quigley, 1991), among others, are the promising approaches in modelling strain localisation.

The model proposed here is based on a homogenisation of shear band and neighbouring intact material and can be classified as an enhanced finite element model. It is similar to the model proposed by Pietruszczak & Mróz(1981) with conditions of equilibrium as well as compatibility condition included in it. We do not attempt to analyse the local behaviour along the shear band, but try to get the overall deformation pattern and load-deformation relations. In this sense, we shall try to simulate the experimental data on intact sandstone(Ord et al., 1991) utilising a homogenisation technique. The onset of localisation, i.e. bifurcation point, will be analysed at the element level. However, it is implicitly assumed here that, if rock masses already contain localised zones in the form of rock joints, the failure would take place through them.

In the following, the bifurcation theory will be reviewed first. It will include the definition of the acoustic tensor, critical hardening modulus and the orientation of bifurcation angle. Next, the homogenisation technique employed right after the bifurcation is summarised. Numerical examples are given to verify the method utilised in this study.

2. Theoretical Background of Bifurcation Problem

As mentioned in the Introduction, the onset of bifurcation is determined at the(finite) element level and, at this point, a homogeneous deformation of a body is no longer possible and non-homogeneous deformation is concentrated on the localised band under the conditions of continuing equilibrium. The remaining portion of the body is assumed to follow the path of an elastic unloading.

The necessary condition for the bifurcation can be derived by employing the kinematic constraint and the equilibrium condition, or equivalently jump condition, across the singular surface(Rice, 1976)

$$\det(n_i D_{ijkl} n_l) = \det(A_{jk}) = 0 \tag{1}$$

for every unit vector(i.e., orientation of the discontinuous surface) n. Here, D_{ijkl} is the usual elasto-plastic matrix relating stress increments to strain increments through

$$\dot{\sigma} = D_{ijkl}\dot{\varepsilon} \tag{2}$$

and A is the acoustic tensor. Eq(1) is equivalent to the loss of ellpticity which is a necessary condition for well-posedness of the boundary value problem. In practice, to find the value of Eq(1) is not so simple since one usually utilises finite load increment. In two-

dimensional problems, Eq(1) becomes quartic and the corresponding bifurcation angle can be found from the minima of the equation.

Critical hardening modulus can be defined as the material characteristics at which bifurcation mode is possible, or the uniqueness of response is not guaranteed. The derivation of the critical hardening modulus is rather tedious and will not be discussed here. When the Mohr-Coulomb yield criterion is employed, the equation by Mandel(1966) is as follows

$$H_{cr} = \frac{G(\sin\phi_m - \sin\psi_m)^2}{8(1-\nu)} \tag{3}$$

where, H_{cr} is a critical hardening modulus, G is a shear modulus, ϕ_m is a mobilised friction angle and ψ_m is a mobilised dilatancy angle. It is noted that H_{cr} is always positive except an associated flow rule. Generally speaking, the bifurcation occurs in the hardening regime, and when the normality rule is valid(i.e., the associated flow rule), the critical hardening modulus can never be positive(Rice, 1976).

Inclination angle of the shear band, θ_c, with respect to the minimum principal stress direction is approximately given by(Vardoulakis, 1980)

$$\theta_c \approx 45^\circ + \frac{1}{4}(\phi_m + \psi_m) \tag{4}$$

It is noted that the angle given in Eq.(4) is the arithmetic average of values given by the classical Coulomb solution, θ_M, and Roscoe's assumption, θ_R, i.e.,

$$\theta_M = 45^\circ + \frac{\phi_m}{2} \tag{5}$$

$$\theta_R = 45^\circ + \frac{\psi_m}{2}$$

3. Application of Homogenisation Technique to Shear Localisation

Once the bifurcation point is detected, shear bands in the appropriate orientations are introduced. The domain of homogenisation will be automatically determined by the size of the finite element. To derive a constitutive relationship of the material having shear band inside, consider a sample intercepted by a shear band inclined at an angle θ having thickness t, length l as shown in Fig. 1. Denote a local coordinate system which is parallel to the shear band as X and a global coordinate system as $\bar{X}$. Assuming a plane strain condition for simplicity, the average stress/strain rate components in constituent materials(i.e., localised interface and nonlocalised material) can be represented by

$$\dot{\sigma}^L = \{\dot{\sigma}_x^L, \dot{\sigma}_y^L, \dot{\tau}_{xy}^L, \dot{\sigma}_z^L\}^T \ : \ \dot{\varepsilon}^L = \{\dot{\varepsilon}_x^L, \dot{\varepsilon}_y^L, \dot{\gamma}_{xy}^L\}^T \tag{6}$$

$$\dot{\sigma}^L = \{\dot{\sigma}_x^N, \dot{\sigma}_y^N, \dot{\tau}_{xy}^N, \dot{\sigma}_z^N\}^T \ : \ \dot{\varepsilon}^N = \{\dot{\varepsilon}_x^N, \dot{\varepsilon}_y^N, \dot{\gamma}_{xy}^N\}^T \tag{7}$$

where, indices N and L denote the nonlocalised and localised zone, respectively. Let homogenised equivalent stress/strain components be represented by

$$\dot{\sigma} = \{\dot{\sigma}_x, \dot{\sigma}_y, \dot{\tau}_{xy}, \dot{\sigma}_z\}^T \ : \ \dot{\varepsilon} = \{\dot{\varepsilon}_x, \dot{\varepsilon}_y, \dot{\gamma}_{xy}\}^T \tag{8}$$

and these can be defined by the following volume averages

$$\dot{\sigma} = \mu_N \dot{\sigma}^N + \mu_N \dot{\sigma}^L \ : \ \dot{\varepsilon} = \mu_N \dot{\varepsilon}^N + \mu_L \dot{\varepsilon}^L \tag{9}$$

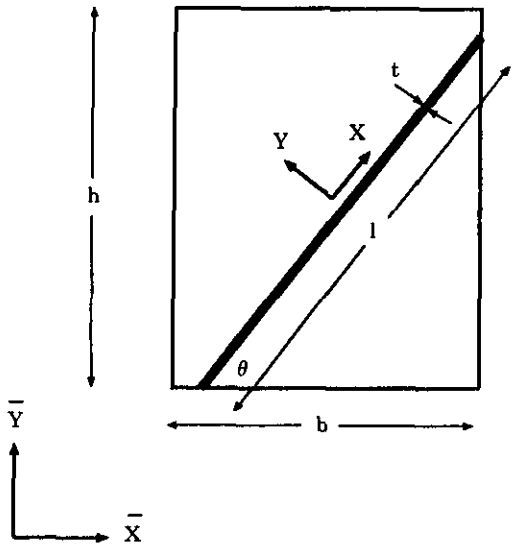

Fig.1 Geometry of shear band with adjacent domain

where, volume fraction of localised zone is $\mu_L = \frac{lt}{A}$, that of nonlocalised zone is $\mu_N = 1 - \frac{lt}{A}$ and $A = bh$. So far, no limitation is imposed on the shape of the element.

Assuming the thickness, t, of the shear band is small compared to the dimension of the element, the following kinematic constraint and equilibrium condition can be established

$$\dot{\varepsilon}_x = \dot{\varepsilon}_x^N = \dot{\varepsilon}_x^L \; ; \; \dot{\sigma}_y = \dot{\sigma}_y^N = \dot{\sigma}_y^L \; ; \; \dot{\tau}_{xy}^N = \dot{\tau}_{xy}^N = \dot{\tau}_{xy}^L \tag{10}$$

Since the thickness of the shear band $t \to 0$, the deformation field can be replaced by the velocity discontinuities, $\dot{g}$,

$$\dot{g} = \{\dot{g}_y, \dot{g}_x\}^T \tag{11}$$

and the averaging rule in eq(9) can be modified into

$$[\delta]\dot{\varepsilon} = [\delta]\dot{\varepsilon}^N + \mu\dot{g} \tag{12}$$

where,

$$[\delta] = \begin{bmatrix} 0 & 1 & 0 \\ 0 & 0 & 1 \end{bmatrix} \; ; \; \mu = \frac{\mu_L}{t} = \frac{l}{A} \tag{13}$$

The stress-strain relations for the constituent materials, i.e., localised and non-localised regimes, may be assumed in the following from :

$$\dot{\sigma}^N = [D]\dot{\varepsilon}^N \; ; \; \dot{\sigma}^L = [K]\dot{g} \tag{14}$$

where

$$[D] = \begin{bmatrix} D_{11} & D_{12} & D_{13} \\ \cdot & \cdot & \cdot \\ \cdot & \cdot & \cdot \\ D_{41} & D_{42} & D_{43} \end{bmatrix} \quad ; \quad [K]^T = \begin{bmatrix} K_{11} \cdot \cdot K_{41} \\ K_{12} \cdot \cdot K_{42} \end{bmatrix}$$

The problem formulated above, viz. Eqs.(9), (10), (12) and (14), is mathematically determinate. The solution can be conveniently expressed in terms of structural matrices relating the strain rates in the constituents to those in the homogenised material;

$$[\delta]\dot{\varepsilon}^N = [S]\dot{\varepsilon} \quad \text{or} \quad \dot{\varepsilon}^N = [S_1]\dot{\varepsilon} \tag{15}$$

Similarly,

$$\dot{g} = [S_2]\dot{\varepsilon} \tag{16}$$

where

$$[S] = ([I]+\frac{1}{\mu}[B])^{-1}([A]+\frac{1}{\mu}[B][\delta])$$

$$[S_1] = \begin{bmatrix} 1 & 0 & 0 \\ S_{11} & S_{12} & S_{13} \\ S_{21} & S_{22} & S_{23} \end{bmatrix} \quad ; \quad [S_2] = \frac{1}{\mu}([\delta]-[S]) \tag{17}$$

$$[A] = \begin{bmatrix} \frac{-D_{21}}{C_1} & \frac{K_{21}}{\mu C_1} & \frac{-D_{23}}{C_1} \\ \frac{-D_{31}}{C_2} & \frac{-D_{32}}{C_2} & \frac{K_{32}}{\mu C_2} \end{bmatrix} \quad ; \quad [B] = \begin{bmatrix} 0 & \frac{K_{22}+\mu D_{23}}{C_1} \\ \frac{K_{31}+\mu D_{32}}{C_2} & 0 \end{bmatrix}$$

$$C_1 = D_{22}+\frac{K_{21}}{\mu} \quad ; \quad C_2 = D_{33}+\frac{K_{32}}{\mu}$$

The constitutive matrix for the homogenised region can be derived directly from the averaging rule, Eq(9),

$$\dot{\sigma} = [D^*]\dot{\varepsilon} \tag{18}$$

where,

$$[D^*] = \mu_N[D][S_1]+\mu_L[K][S_2] \approx [D][S_1] \tag{19}$$

assuming $\mu_L \to 0$. With reference to $\overline{X}-\overline{Y}$ coordinate system,

$$\dot{\sigma} = [T]\dot{\overline{\sigma}} \; ; \quad \dot{\varepsilon} = [T_1]\dot{\overline{\varepsilon}} \tag{20}$$

and

$$\dot{\overline{\sigma}} = [T]^{-1}[D^*][T_1]\dot{\overline{\varepsilon}} \tag{21}$$

where $[T]$ and $[T_1]$ are the appropriate transformation matrices.

It should be noted that the mechanical behaviour of the homogenised material does not depend on the thickness of the shear band which has been formally eliminated from macroscopic considerations. Also, the position of the shear band within the element is not important since the homogenisation is performed according to the volume fractions of the constituents.

A shear band is basically an interface, and constitutive relations similar to those used for rock joints can be similarly applied to the shear band. Therefore, the constitutive equations of the shear band in the elastic range can have the form

$$[\delta]\dot{\sigma}^{L} = [K^{e}]\dot{g} \tag{22}$$

with

$$[K^{e}] = \begin{bmatrix} K_N & 0 \\ 0 & K_S \end{bmatrix} \; ; \; \dot{\sigma}_x^{L} = \dot{\sigma}_z^{L} = \alpha\dot{\sigma}_y^{L} \tag{23}$$

where K_N and K_S are the normal and shear components of the elastic stiffness and

$$\alpha = 1 - \frac{2K_s}{K_N}$$

Adopting an elasto-plastic description of the shear band, the yield function and the plastic potential functions are defined as

$$F = F(\sigma_y^{L}, \tau_{xy}^{L}, \kappa) = 0 \; ; \; Q = Q(\sigma_y^{L}, \tau_{xy}^{L}) = \text{const.} \tag{24}$$

where,

$$\kappa = \kappa(g^{p}) \; ; \; \dot{g}^{p} = \dot{\lambda}[\delta]\frac{\partial Q}{\partial \sigma^{L}} \tag{25}$$

and $[\delta]$ is defined in Eq. (13). Following the standard plasticity procedure, the constitutive law may be expressed in the form analogous to that of Eq.(23), i.e.

$$[\delta]\dot{\sigma}^{L} = [K^{ep}]\dot{g} \tag{26}$$

where,

$$[K^{ep}] = \begin{bmatrix} K_{11} & K_{12} \\ K_{21} & K_{22} \end{bmatrix} \tag{27}$$

In the next, Mohr-Coulomb yield criterion with non-associated flow rule, which may be appropriate to the rock material, will be employed and the following deviatoric hardening/softening rule similar to Pietruszczak(1992) is considered to model the shear band behaviour

$$\tan\phi_m = \tan\phi_r - (\tan\phi_r - \tan\phi_i)\exp[-C_0 g_x^{p}(g_x^{p} + C_1)] \tag{28}$$

where, ϕ_i is the initial friction angle which may be the same as the friction angle of the intact material, ϕ_r is the residual friction angle which is calculated from

$$\phi_r = C_2\phi_i \tag{29}$$

and ϕ_m is the mobilised friction angle. C_0, C_1 and C_2 are material constants. The mobilised dilatancy angle is similarly defined by using a direct relationship with the material constants for intact material.

4. Numerical Example

In this Section, numerical studies regarding the shear localisation are illustrated through the utilisation of the homogenisation technique. Specifically, compression of a rock specimen is simulated according to the experimental data given in Ord, et. al. (1991). The material properties used in the example are shown in Table 1 and the geometry as well as boundary conditions are described in Fig. 2. Also shown in Fig. 2 is the constant confining pressure, $q_0 = 0.015$ KPa. The material parameters needed for the modelling of shear band are the normal as well as shear stiffinesses, K_N & K_s, constants for the deviatoric hardening / softening rule, C_0, C_1 & C_2.

As is well known, when the finite element method is used to analyse the localisation or the strain softening behaviour, the results are usually mesh dependent. To overcome this deficiency, several attempts have been made during last decade.

Especially, these attempts tried to employ the idea of the length scale or localisation limiter. In this study, the shear bands have been smeared or homogenised into the finite elements and, therefore, the results show the mesh independent behaviour unless very crude

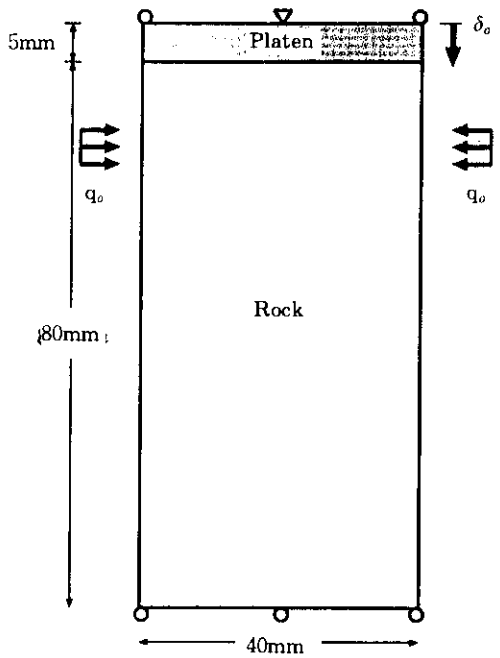

Fig.2 Geometry and boundary conditions of example

Table 1 : Material Properties used in Example

Rock specimen		
Dimension	W × H	40 × 80mm
Young's modulus	E_i	12.1×10^6 KPa
Poisson's ratio	ν_i	0.31
Cohesion	C_i	1.0×10^4 KPa
Friction angle	ϕ_i	44°
Dilatancy angle	ψ_i	20°
Steel pad		
Thickness	t_s	5.0mm
Young' modulus	E_s	30.0×10^6KPa
Poisson's ratio	ν_s	0.30
Shear band		
Normal stiffness	K_N	$1.677 \frac{KPa}{mm}$
Shear stiffness	K_s	$0.462 \frac{KPa}{mm}$
Cohesion of shear band	C_j	4.0×10^3 KPa
Residual dilatancy angle	ψ_r	10°
Material constant	C_0	1.0mm
Material constant	C_1	1.0×10^{-4}mm
Material constant	C_2	0.7

meshes are used. Specifically, 4 finite element mesh designs(66, 153, 231 & 325 elements) with the same mesh design and with the same material parameters(Table 1) have been considered to test the mesh dependencies and, except a coarse mesh, the mesh objectivity is clearly demonstrated. See Fig. 3. It is noted from Fig. 3 that the peak load is essentially the same in all cases and, except for the mesh with 66 elements, the overall load-displacement curves show the same patterns. Meanwhile, Fig. 4 illustrates the development of shear localisation in a mesh with 231 elements and it shows that the localisations start in the middle of the specimen even though an initial disturbance occurs near the upper left corner due to biased mesh configuration. The remaining meshes also show the same localised pattern except coarse mesh(66 elements) and, in this case, the final development of localisation is expected when the prescribed displacement is further increased.

In the above, the biased meshes as well as steel pad were used to initiate the shear localisation. However, if one employs the uniform meshes, the results are significantly different from the previous ones. For example, up to $\delta_0 = 0.83$mm, symmetric shear localisations are developed with 210 uniform elements. If the loads are further increased, the deformed shape will be eventually unsymmetric and localised mode can be realised, mainly due to the numerical round-off errors. A weak element in which the cohesion of intact rock, C_i, is reduced by 20% is then introduced near the upper right boundary of the specimen. As expected, the shear localisation is initiated from the weak element and propagated downward. The load−displacement curves in these cases are shown in Fig. 5. Also shown is the

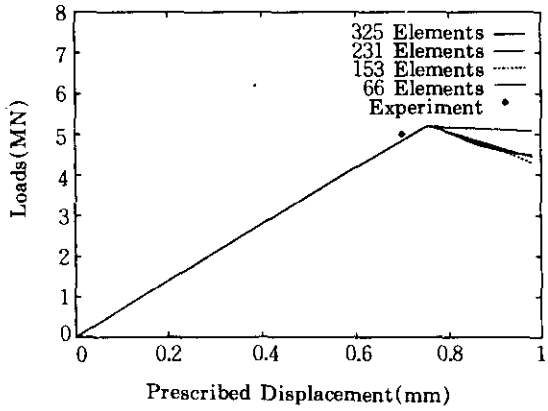

Fig.3 Load-displacement curve with varying number of elements

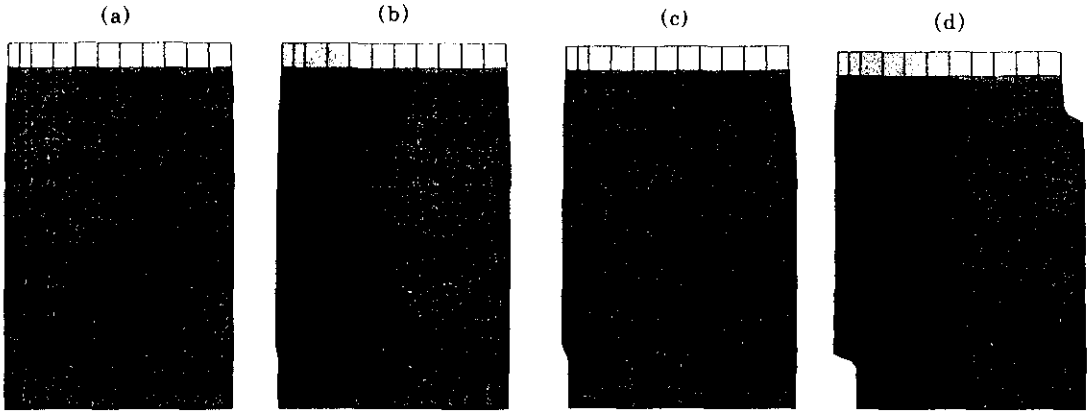

Fig.4 Displacement pattern with 231 elements
(a) δ_o=0.760mm (b) δ_o=0.770mm
(c) δ_o=0.780mm (d) δ_o=0.830mm

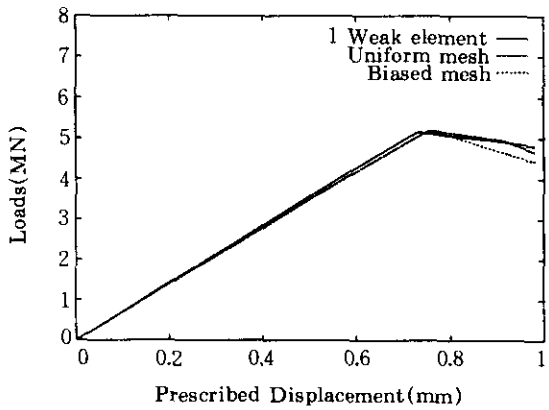

Fig.5 Load-displacement curve with various mesh designs

case of biased meshes(231 Elements) for comparison. Up to the peak load, the behaviour of uniform or weak element meshes is basically the same as biased meshes. However, in the post-peak region, the softening of the specimen seems to be delayed.

5. Conclusions

In this paper, enhanced finite element model has been proposed to capture the localised shear band of the geomaterial. The material was initially assumed to be intact and subsequently discontinuous due to the bifurcation or shear localisation. A homogenisation technique has been applied after the bifurcation at the integration point, where a weak (band) material, i.e., a shear crack or an interface, is artificially generated and smeared over the finite element. Specifically the following conclusions can be made :

- Artificial equivalent material properties are derived on the basis of proposed homogenisation technique. These are used when the stress state at the Gauss point reaches bifurcation point.
- A deviatoric softening rule is employed to model the post-peak behaviour of the shear band.
- Through the parametric studies, it is demonstrated that the results are mesh-independent unless, of course, very coarse meshes are used which would naturally give different results due to crude discretisation.

One of the advantages of the proposed technique studied here is in its simplicity. Neither additional degrees of freedom nor a special shape function is introduced to analyse the shear localisations. However, it is noted that, to get a good result, very small value of the convergence tolerance has to be adopted when calculating the norm of the equivalent nodal forces.

References

1. Borst, R. D. and Pamin, J. (1996), "Some Novel Developments in Finite Element Procedures for Gradient-Dependent Plasticity", I. J. Num, Meth. Eng., 39, 2477-2505.
2. Borst, R. D., Sluys, L. J., Mühlhaus, H.-B. and Pamin, J. (1993), "Fundamental Issues in Finite Element Analyses of Localization of Deformation", Eng. Comp., 10, 99−121.
3. Loret, B. and Prevost, J. H. (1990), "Dynamic Strain Localization in Elasto−(Visco) Plastic Solids, Part I. General Formulation and One-Dimensional Examples", Comp. Meth. Appl. Mech. Eng., 83, 247−273.
4. Mandel, J. (1966), "Conditions de Stabilité et Postulat de Drucker", in J. Kravtchenko and P. M. Sirieys(eds.), Proc. IUTAM Symp. Rheology and Soil Mech., pp.58−68.
5. Ord, A., Vardoulakis, I. and Kajewski, R. (1991), "Shear Band Formation in Gosford Sandstone", I. J. Rock Mech. Min. Sci. & Geomech. Abstr., 28, 397−409.
6. Ortiz, M. and Quigley, J. J. (1991), "Adaptive Mesh Refinement in Strain Localization Problems", Comp. Meth. Appl. Mech. Eng., 90, 781−804.
7. Papanastasiou, P. C. and Vardoulakis, I. G. (1992), "Numerical Treatment of Progressive Localization in Relation to Borehole Stability", I. J. Num. Anal. Meth. Geomech, 16, 389−424.

8. Pietruszczak, S. and Mróz, Z.(1981), "Finite Element Analysis of Deformation of Strain-Softening Materials", I. J. Num. Meth. Eng., 17, 327−334.
9. Pietruszczak, S. and Niu, X. (1992), "Numerical Evaluation of Bearing Capacity of a Foundation in Strain Softening Soil", Comp & Geotech., 13, 187−198.
10. Rice, J. R. (1976), "The Localization of Plastic Deformation", in W. T. Koiter(ed.), 14th IUTAM Congr. : Theo. and Appl. Mech., pp.207−220.
11. Steinmann, P. and Willam, K. (1991), "Performance of Enhanced Finite Element Formulations in Localized Failure Computations", Comp. Meth. Appl. Mech. Eng., 90, 845−867.
12. Vardoulakis, I. (1980), "Shear Band Inclination and Shear Modulus of Sand in Biaxial Tests", I. J. Num. Anal. Meth. Geomech., 4, 103−119.

(received on Apr. 9, 1997)